Cell and Tissue Research
September 2022, Volume 390, Pages 358-398
https://doi.org/10.1007/s00441-022-03675-0
https://archimer.ifremer.fr/doc/00792/90427/

Ontogenetical development of branchial chambers of *Litopenaeus vannamei* (Boone, 1931) and their involvement in osmoregulation: ionocytes and Na+/K+-ATPase

Chong-Robles Jennyfers [1, *], Giffard-Mena Ivone [1], Patrón-Soberano Araceli [2], Charmantier Guy [3], Boulo Viviane [4], Rodarte-Venegas Deyanira [5]

[1] Facultad de Ciencias Marinas, Universidad Autónoma de Baja California (https://ror.org/05xwcq167), Ensenada, Baja California, Mexico
[2] División de Biología Molecular, Instituto Potosino de Investigación Cientifica y Tecnológica, San Luis Potosí, Mexico
[3] Marbec, Université de Montpellier, CNRS, Ifremer, IRD, Montpellier, France
[4] IHPE, Université de Montpellier, CNRS, Ifremer, Université de Perpignan Via Domitia, Montpellier, France
[5] Facultad de Ciencias, Universidad Autónoma de Baja California (https://ror.org/05xwcq167), Ensenada, Baja California, Mexico

* Corresponding author : Jennyfers Chong-Robles, email address : jennyfer.chong@gmail.com

Abstract :

Branchial chambers constitute the main osmoregulatory site in almost all decapod crustaceans. However, few studies have been devoted to elucidate the cellular function of specific cells in every osmoregulatory structure of the branchial chambers. In decapod crustaceans, it is well-known that the osmoregulatory function is localized in specific structures that progressively specialize from early developmental stages while specific molecular mechanisms occur. In this study, we found that although the structures developed progressively during the larval and postlarval stages, before reaching juvenile or adult morphology, the osmoregulatory capabilities of Litopenaeus vannamei were gradually established only during the development of branchiostegites and epipodites, but not gills. The cellular structures of the branchial chambers observed during the larval phase do not present the typical ultrastructure of ionocytes, neither Na+/K+-ATPase expression, likely indicating that pleura, branchiostegites, or bud gills do not participate in osmoregulation. During early postlarval stages, the lack of Na+/K+-ATPase immunoreactivity of the ionocytes from the branchiostegites and epipodites suggests that they are immature ionocytes (ionocytes type I). It could be inferred from IIF and TEM results that epipodites and branchiostegites are involved in iono-osmoregulation from PL15, while gills and pleura do not participate in this function.

Keywords : Ontogeny, Postlarvae, Shrimp, Salinity adaptation, Hypo-osmoregulation, Mitochondria-rich cell

Introduction

Osmoregulation is a key adaptive physiological process to deal with salinity variations (Péqueux 1995; Charmantier 1998). By this process, animals regulate their blood or hemolymph osmolality according to their particular physiology. Crustaceans can be osmoconformers, hypo, or hyper-regulators depending on the species (Gilles and Pequeux 1981); some of them have behavioral patterns related to reproduction and development, which expose the organism at successive ontogenetic stages to different salinity regimes (Anger 2001). According to Charmantier (1998), crustaceans have developed three ontogenetic osmoregulatory patterns closely linked with their life cycles.

The hemolymph osmolality regulation in crustaceans depends on the osmoregulatory behavior (Mantel et al. 1983). To do that, crustaceans can use intracellular osmotic effectors (e.g., amino acids), modify the area and permeability of the surface membranes for exchanges (as a limiting strategy), or compensate for the gain or loss of ions by an active transport mechanism (compensatory strategy) (Mantel et al. 1983). During the ontogeny of marine crustaceans, the osmoregulation is based mainly on the active transport mechanisms to regulate the ionic concentration of Na^+ and Cl^- (Charmantier 1998). However, when and where this osmoregulatory strategy is established during ontogeny of crustaceans is poorly known.

The osmoregulatory active transport mechanisms have been localized mainly in structures of the branchial chambers (Bouaricha et al. 1994; Lignot and Charmantier 2001; Cieluch et al. 2004, 2005; Boudour-Boucheker et al. 2013; Pham et al. 2016) and the excretory glands (BoudourBoucheker et al. 2013). The branchial chamber is formed by pleura (cephalothoracic body wall), and branchiostegite, with gills and epipodites inside this chamber. There is a branchial chamber in each dorso-anterior side of the shrimp body. The different components of the branchial chambers are in close contact with the environment to function as osmoregulatory effectors in response to any salinity change (Péqueux et al. 2006).

The osmoregulatory function in crustaceans is achieved with the development of epithelia characterized by the presence of ionocytes (Charmantier 1998). These cells present membrane modifications to increase the interchange with the environment and to allow the allocation of different molecular mechanisms. A typical crustacean ionocyte is characterized by membrane modification called microvilli on the apical side and deep invaginations associated with many mitochondria on its basal side (Bouaricha et al. 1991; Péqueux 1995). Ion transports by ionocytes are performed by complex molecular mechanisms driven chiefly by the Na^+/K^+-ATPase pump (NKA) and other transporters that contribute to iono-osmoregulation (e.g., K^+, Na^+, Cl^- channels, $Na^+/K^+/2Cl^-$ cotransporter, Na^+/H^+ exchanger, Cl^-/HCO_3^- antiporter, carbonic anhydrase, and in general the H^+-type V ATPase) (Freire et al. 2008; McNamara and Faria 2012).

The ionocytes and NKA-based molecular mechanisms have been largely described in juvenile and adult crustaceans, but less attention has been focused on the younger developmental stages and on the development of each structure of the branchial chamber. The few available investigations suggest that the osmoregulatory function begins during early development; however, the role of each structure during ontogeny varies between crustacean groups (e.g., crabs vs. lobster or shrimp). For example, Cieluch et al. (2004) have found in the megalopa stage crab of *Carcinus maenas* that osmoregulatory function is established only on the posterior gills as soon as the gills were developing. In contrast, in the lobster *Homarus gammarus*, osmoregulation is performed by the pleura during larval stages, but the epipodites and branchiostegites take over this function in juvenile and adult stages (Lignot and Charmantier 2001). Similar observations have been reported in shrimps such as *Macrobrachium amazonicum* (Boudour-Boucheker et al. 2014), *Crangon crangon* (Cieluch et al. 2005), and in the peneid shrimps *Penaeus japonicus* (Bouaricha et al. 1994) and *Litopenaeus stylirostris* (Pham et al. 2016). To date, no study has been conducted on the role of the different branchial chamber structures in osmoregulation during the ontogeny of one of the most popular species cultivated around the world, the shrimp *Litopenaeus vannamei*.

L. vannamei have a larval ontogeny type III osmoregulatory pattern (Chong-Robles et al. 2014) similar to other penaeids such as *P. japonicus* (Bouaricha et al. 1994) and *L. stylirostris* (Pham et al. 2012). In this pattern, metamorphosis marks the appearance of the adult type of osmoregulation (Charmantier 1998). *L. vannamei* has a complex life cycle comprising a pelagic larval phase and a benthic juvenileadult phase (FAO 2004). Their development comprises during the larval phase six naupliar stages (N1–6), three zoea (zoea 1–3), three mysis (mysis 1–3), and then several postlarval stages turning into juveniles and adults (Kitani 1986). Juvenile and adult stages are euryhaline in their natural environment (FAO 2004) (ecological euryhalinity), while the other developmental stages can be considered relatively euryhaline (Péqueux et al. 2006) as they have been studied only under experimental conditions. All stages tolerate salinities between 20 and 45 PSU, but there is an increase in the tolerance of low salinities (10 and 5 PSU) at PL2 and PL4, respectively; high salinity tolerance (60 PSU) begins from PL15. Mysis stages of *L. vannamei* are osmoconformers or slightly hyper-osmoregulators in salinities

from 20 and 45 PSU, while starting from postlarvae 1 stage, these young shrimps are hypo-osmoregulators at high salinity (≥ 32 PSU) and hyper-osmoregulators at low salinity (≤ 20 PSU). *L. vannamei* has a slightly wider salinity tolerance compared to *L. stylirostris* or *P. japonicus* (Chong-Robles et al. 2014). However, other aspects of the ontogeny of osmoregulation remain unknown; the development and the osmoregulatory function of the branchial chambers are among the unknown issues.

The aim of this work is to describe the development of the branchial chamber from selected developmental stages of *L. vannamei* exposed to 32 PSU. We evaluated the osmoregulatory function by InmunoIndirect Fluorescence (IIF) Na^+/K^+-ATPase (NKA) staining and confirmed the presence of ionocytes by transmission electron microscopy (TEM). A description of pleura, gills, branchiostegite, and epipodite development is provided.

Materials and methods

Sample preparation

Litopenaeus vannamei at different developmental stages were supplied by AQUAPACIFIC shrimp hatchery. The larval developmental stages (nauplii to mysis) were assigned according to Kitani (1986); each postlarval (PL) stage measuring between 5 ± 0.005 and 12 ± 0.33 mm corresponds to 1 day forward culture until animals reach 1 g weight as indicative of the juvenile stage (FAO 2004). The C molt stage was visually verified in juveniles and adults according to Rodríguez-Pérez et al. (2006). Plastic containers of different sizes were used according to animal size (from 1 to 600 L) and filled with 32 PSU (941 mOsm/kg) natural seawater at 25 ± 0.5 °C (adjusted with 200-W titanium electric heaters) with constant aeration. All shrimps were unfed during the experiment.

Different techniques were used to describe branchial chamber morphology. At least ten specimens were fixed depending on type sample requirement. For light microscopy (LM) and indirect immunofluorescence (IIF), shrimps were fixed in Davidson solution according to Lightner (1996), larvae and postlarvae for 12 h, and juveniles and adults for 24 h, and then preserved in 70% ethanol. For transmission electron microscopy (TEM), mysis 2 and PL1 were whole preserved, while small pieces of branchiostegite and the epipodites from PL15, juvenile, and adult were dissected (only those from gills associated to the 3rd pereiopod were taken). TEM samples were fixed for 12 h in 2% glutaraldehyde adjusted with 0.1 M sodium cacodylate buffer according to the animal osmotic pressure (with the addition of NaCl). Samples were then preserved in 1% glutaraldehyde until complete processing for TEM. The osmotic pressures of animals and seawater were measured as has been previously described (Chong-Robles et al. 2014).

Branchial chamber morphology

The branchial chamber was observed in several developmental stages (zoea, mysis, PL1–PL6, PL9–PL13, PL15, PL22, PL39, juvenile, and adult). Animals preserved in 70% ethanol for LM were delicately washed in distilled water and mounted on a small Petri dish. Larvae and postlarvae were stained 1 min with methylene blue (1%) and immersed in immersion oil to facilitate observation and manipulation. Animals (larvae and postlarvae, $n = 10$ animals each; juvenile and adult, $n = 5$ animals each) were carefully dissected under a stereoscopic microscope. The organisms were transversely excised, the branchiostegite were removed, and the gills and epipodites were counted and photographed to follow the development of their morphology.

Additionally, organisms at PL1–PL4 and PL22 stages previously preserved in glutaraldehyde 1% in cacodylate buffer were processed for scanning electron microscopy (SEM). Afterward, the organisms were postfixed with 1% OsO_4 in a buffer for 1 h at 4 °C. The samples were gradually dehydrated with absolute ethanol from 30 to 100% for 30 min with each concentration and washed twice with 100% absolute ethanol, each washing lasting 1 h. The critical point drying process was performed in a Tousimis Samdri-PVT- 3D, and the dry samples were mounted to perform the gold sputter coating in a Cressington apparatus model 108 auto and examined in a FEI model Quanta 200 SEM. SEM was adjusted at 25 kV, spot 4.5, and WD 10 mm, taking the micrographs with a back-scattering detector (BSD).

Cell topography and NKA localization

The Na^+/K^+-ATPase (NKA) and ionocyte presence are critical factors determining the osmoregulatory cell function in crustacean's tissues. In this study, techniques like the hematoxylin–eosin (H&E) staining, IIF, and TEM were used to assess the branchial chamber osmoregulatory function in different developmental stages of *L. vannamei*.

Briefly, for H&E and IIF techniques, each animal was cut transversally and longitudinally in 4-µM sections; they were separated in A and B series. The A-series was immersed in an egg albumin water bath at 35 °C and collected on slides; they were dried for 2 days at ambient temperature and stored in slide boxes until processed for H&E staining. The B-series was directly collected on poly-ı-lysine-coated slides (0.1%), dried for 2 days at 35 °C, and preserved at 4 °C until analyzed for IIF.

The H&E staining was made in five animals for each developmental stage (zoea 3, mysis 1–3, PL1–2, PL4, PL7–8, PL12, PL15, PL22, PL39, juvenile, and adult) following routine laboratory technique. The IIF was made in three animals of selected stages of development (zoea 3, mysis 1–3, PL1, PL4, PL15, juvenile, and adult). For these samples, the slides were pre-warmed at 45 °C for 30 min, deparaffinized in xylene butanol, and gradually hydrated through a decreasing ethanol series (100%, 90%, 70%, 50%). Afterward, the sections were rehydrated with phosphate buffer saline (PBS), pH 7.3 for 5 min, permeabilized with a 0.2% Tween 20 in PBS for 10 min, and then blocked with 5% skimmed milk (SM)-PBS for 20 min. To remove residual blocking solution, slides were washed (3 × 5 min) with PBS before incubation for 2 h at room temperature with a PBS-diluted primary antibody (10 µg/mL) against α5- Na^+ -K^+-ATPase, a mouse anti-chicken antibody (α5-NKA, University of Iowa, Hybridoma Bank) previously shown to detect several isoforms of NKA in fish and crustaceans (Charmantier et al. 2009). As a negative control for background staining, selected slides were incubated for 2 h at room temperature with PBS lacking primary antibody. The sections were then washed (3 × 5 min) with PBS before incubation with a fluorescein isothiocyanate (FITC)–conjugated goat anti-mouse secondary antibody (10 µg/mL; Jackson ImmunoResearch) for 1 h at room temperature. After that, the slides were washed (3 × 5 min) with PBS. Sections were examined using a FITC filter on a Zeiss Axioskop 40 epifluorescence microscope with a digital camera (Carl Zeiss Microimaging, Inc., NY, USA).

Cell ultrastructure

The cell ultrastructure was observed from dissected pieces of gills (PL15, juvenile, adult), branchiostegites (mysis 2, PL1, PL15), and epipodites (PL1, adult). Samples previously preserved in 1% glutaraldehyde were postfixed in 1% OsO_4 for 1 h on ice. The tissues were washed and dehydrated in increasing ethanol concentrations. The inclusion was done in LR White resin (Ted Pella) gradually changed to 3:1 ethanol/ resin, 1:1 ethanol/resin to overnight pure resin, and one last changed with pure resin in a rotating device for 3 h. Then, the tissues were polymerized for 2 days in a UV chamber. Semi-thin sections for light microscopy were stained with toluidine blue. Ultra-thin Sects. (75 ± 15 nm) were cut with a diamond knife on an ultramicrotome (Sorvall MT2) and placed on FCF-100 Cu. They were contrasted using aqueous uranyl acetate (2% w/v) and aqueous lead citrate (2% w/v). Samples were examined on a JEM-200 CX (JEOL) transmission electron microscope at 100 kV, equipped with a digital camera (SIA, Germany) to record selected images.

Results

Branchial chamber development

An incipient chamber formed between branchiostegite and pleura was observed at the zoea stage, but neither gills nor epipodites were developed (Fig. 1a). The different structures forming branchial chamber developed as follows:

Pleura: Pleura are flattened structures that cover the lateral anterior part of the body on both sides. They internally limit each branchial chamber. In the early developmental stages of *L. vannamei* (zoea and mysis), the pleura was formed by a simple epithelium formed by cubic cells and protected by a cuticle (Fig. 2). This epithelium progressively flattened in later stages until appearing as a layer of flat cells almost undetectable in postlarval stages. Branchiostegites: These structures are the lateral side of the cephalothorax. They externally limit each branchial chamber. They were formed by

two epithelia, each facing the inner or the exterior side and each covered by cuticle. In larval stages, both epithelia were formed by cubic cells with similar thickness and protected by a similar cuticle. However, these epithelia were progressively modified until being completely different as can be seen in Fig. 3. At PL15, the inner epithelium was markedly thicker, while the external side was characterized by cubic cells with a thick cuticle (Fig. 3a). These characteristics were more remarkable at PL39 (Fig. 3b) and in the juvenile stage (Fig. 3c); the inner side of the structure was characterized by a thin cuticle associated with epithelium of cells higher than those located in the outer side of the structure.

Gills: The gill development in L. vannamei begun as little buds during mysis stages (Fig. 2). These tiny gills are arthrobranch gills, which grew like paired structures with a tubular shape just above the thoracic appendages with a dorsolateral orientation (Fig. 1b). The first gill ramifications were observed at PL2-PL4. The ramifications and gills number increased until the development of eleven arthrobranchs and seven pleurobranchs in the PL11 stage. During the gills' development, first grew the arthrobranch in pairs (except the last one) and posteriorly the pleurobranchs, after PL10 stage. The pairs of arthrobranch were inserted on each coxa from the 2nd maxilliped to the 3rd pereiopod; the last arthrobranch gill was located in the 4th pereiopod. The pleurobranchs were situated on the pleura on each one of the seven appendices. However, it was not until latter postlarval stages (> PL15) that gills acquired a dendrobranchiata morphology typical of penaeid shrimps. The cell topography of gills in mysis stage shows a structure formed by a simple epithelium with an incipient septum dividing the hemolymph circulation and protected by a cuticle (Fig. 2). The cubic epithelium was continually flattening out to form a thin epithelial layer. These cells are separated by a space between two contiguous cells through extensions of the cytoplasm, creating the hemolymphatic lacunae. The gills were divided by septa of conjunctive tissue, which split gills (at any level of ramification) into afferent and efferent vessels for the hemolymph circulation (Fig. 2).

Epipodites: A first epipodite was observed from PL1. The structure grew quickly in later developmental stages, and it was clearly distinguished from gills in the PL4 stage (Fig. 1c). The development of the other epipodites was only observed in later stages; for instance, PL10 and PL11 had either one, two, or five epipodites, suggesting epipodite retention and a variable growth of these structures during these postlarval stages (Fig. 1d). All individuals observed at PL15 stage and in older stages had five epipodites (Fig. 1f). Epipodites were morphologically flat lobed structures that changed to well-developed flat bilobed structures, Y-shaped with setae at the juvenile and adult stages (Fig. 1f). The five epipodites were localized at the basis of the coxa from the 2nd maxilliped to the 3rd pereiopods. At the cellular level, epipodites during early postlarval stages were limited by an epithelium formed by cubic cells covering all the structures (Fig. 3d). This cubic epithelium progressively lengthened until the cells were prismatic at the PL15 (Fig. 3e), juvenile (Fig. 3f), and adult stages (not shown). As can be seen in Fig. 3d–f, both sides of the structure were formed by the same type of epithelium limiting hemolymphatic lacunae.

Figure 4 outlines the development of those structures forming the branchial chamber.

Evaluation of branchial chamber osmoregulatory function through IIF

The osmoregulatory function into the branchial chamber of *L. vannamei* was evaluated through InmunoIndirect Fluorescence (IIF) N a^+/K^+-ATPase (NKA) staining and by transmission electron microscopy (TEM) in selected developmental stages. In the larval stages of *L. vannamei*, there was no evidence of NKA immunolocalization (Table 1). In addition to the lack of immunolocalization observed in the mysis stage (Fig. 5a), the observation of the cell ultrastructure in the epithelia forming the branchiostegite (Fig. 5b) and pleura (Fig. 5c) at that stage revealed that these cells observed did not have any modifications on the basal or apical side, either mitochondria or membrane modifications.

The first evidence of osmoregulatory epithelia in *L. vannamei* was observed at the first postlarval stage with the presence of ionocytes in the branchiostegite and the epipodite. In the branchiostegites, cells with features typical of ionocytes were found only in the epithelium covering the inner side of the structure, while in the epipodites, they were located in the epithelium covering all structure. In both structures, the ionocytes were mitochondria-rich cells (MRC) mainly on the basal side; on the apical side of the branchiostegites, the apical evaginations were shorter than the apical evaginations observed in the ionocytes of epipodites (Fig. 6a, b, d). In Fig. 6c, cells connecting both sides of the branchiostegite were observed, suggesting the presence of pilaster cells (Taylor and Taylor 1992) with mitochondria on the basal side and evaginations on

the apical side, possibly functioning like ionocytes. Even with this MRC-like ultrastructure, IIF did not show NKA immunolabeling in the PL1 stage or in any early postlarval stage evaluated until PL15 (Table 1).

Evidence for osmoregulatory involvement was enhanced at older postlarval stages, as shown by the NKA immunolocalization at PL15 stage, juvenile, and adult stage (Table 1). Control sections without the primary antibody showed no NKA immunolabeling (not shown). The NKA immunolabeling was positive in branchiostegite and epipodite cells from PL15 stage (only epipodite shown; Fig. 7a), and juvenile (Fig. 7b) and adult stage (no show). NKA was specifically localized on the basolateral membrane of the ionocytes where the mitochondria were localized (Fig. 7c, d). In contrast to cells forming branchiostegites and epipodites, IIF did not show any immunolabeling of NKA in cells forming gills or pleura in any developmental stage evaluated (Table 1; Fig. 7).

The NKA immunolocalization observed through IIF was corroborated by the presence of well-developed ionocytes observed through TEM in the branchiostegites and epipodites. In the branchiostegite, TEM revealed cells with welldeveloped apical evaginations and numerous large mitochondria forming clusters on the basal side (Fig. 6e–g). In the epipodite, the ionocytes had many large mitochondria on the basal side, but these organelles were also found on the apical side associated with a few short evaginations (illustrated for the adult stage; Fig. 6h, i). Consistent with IIF, gill cells observed by TEM analysis did not present ionocyte
features either in the lamella or septum at PL15 (Fig. 8a) or at the juvenile (Fig. 8b, c) or adult stage (Table 1).

Discussion

Branchial chambers in crustaceans are formed of different components: pleura (cephalothoracic body wall), branchiostegite, gills, and epipodites (Mantel et al. 1983). Previous studies in crustaceans have demonstrated that the involvement of the branchial chambers in ion transport and therefore in the osmoregulatory function starts and increases according to the development and differentiation of their anatomical and cellular components (Lignot and Charmantier 2001; Cieluch et al. 2004, 2005; Boudour-Boucheker et al. 2013; Pham et al. 2016). The contribution of each structure to active ion transport and osmoregulation varies between species and salinity during ontogeny; also, in some species, a transition of the iono-osmoregulatory function between structures during the development has been reported. The majority of these studies have been focused on the detection of the iono-osmoregulatory epithelia, and less attention has been paid to the complete development of the branchial chamber. In this study, we describe the branchial chamber of *L. vannamei*; we also identify structures presenting typical features associated with ion transport, such as cell ultrastructure of an ionocyte (membrane modifications and mitochondria) and NKA expression, in selected developmental stages from zoea to adult.

A summary of our findings is presented in Table 1. We found that the osmoregulatory capability of *L. vannamei* was gradually established during the development of the branchiostegites and epipodites. It could be inferred therefore from IIF and MET results that gills and pleura do not have a role in ion transport linked to iono-osmoregulation. The absence of immunoreactivity of the ionocytes from the branchiostegites and epipodites during early postlarval stages suggests that they were immature ionocytes (ionocytes type I), which reached complete differentiation for ion transport at least at PL15 when also *L. vannamei* has all epipodites completely developed.

Branchial chamber development

During the early larval stages of *L. vannamei*, only the pleura and branchiostegite were developed. These structures formed incipient open branchial chambers similar to the open branchial chambers described in other decapods with similar body anatomy containing gills inside two chambers in adults (Bauer 1999) such as the lobster *Homarus gammarus* (Lignot and Charmantier 2001) and shrimps like *Penaeus japonicus* (Bouaricha et al. 1994), *Crangon crangon* (Cieluch et al. 2005), *Macrobrachium amazonicum* (Boudour-Boucheker et al. 2013), and *Litopenaeus stylirostris* (Pham et al. 2016). The onset of gills and epipodite in *L. vannamei* occurs during the mysis stage, in line with those reported in penaeid shrimp, *P. japonicus* (Bouaricha et al. 1994), and *L. stylirostris* (Pham et al. 2016). But the timing is different in other species: for example, in the lobster *H. gammarus*, the gills and epipodites start developing since early embryonic stages (Lignot and Charmantier 2001), in the shrimp *M. amazonicum* during the zoea V stage (Boudour-Boucheker et al. 2013), and in *C. crangon* during the first decapodite (Cieluch et al. 2005). Differences between the beginning of the development of these

structures could be attributable to their different patterns of larval development since in *L. vannamei* (and in other penaeid shrimp belonging to the dendrobranchiata suborder); it includes free-living (planktonic) naupliar stages, three zoea stages, and three types of mysis stages before the metamorphosis to juveniles. Comparatively, the development in the Pleocyoemata suborder (*M. amazonicum*, *H. gammarus*, *C. crangon*) does not include free-living naupliar stages: The hatching larva is a zoea, followed by a variable number of zoea l stages then a metamorphosis to decapodite/postlarval/ juvenile stages (Anger 2001).

In our study, we found that the shape of gills and epipodites was gradually changing during early postlarval stages (PL1–PL15), while the pleura and branchiostegite only changed in size according to the animal growth. The primary gills that were observed as buds at the mysis stage began to branch up in the PL1 stage, when also one epipodite was observed. It is noteworthy that between the PL4 and PL6 stage, eleven gills were present, but only one epipodite was still developed; although gills were gradually emerging and developed during the next postlarval stages, the epipodites were observed as buds between PL10 and PL11 stages, which suggests epipodite retention as reported by Bouaricha et al. (1994) in *P. japonicus*. The full number of epipodites (5) in *L. vannamei* was completed at the PL15 stage. The epipodite retention lasted longer than reported in *P. japonicus*; it lasts approximately from mysis to the PL5 stage (Bouaricha et al. 1994). Epipodite retention is an interesting finding as it rules out the possibility that these structures have their main role in hyper-osmoregulation. In addition, we also observed that the typical morphology of dendrobranchiate gill in penaeid shrimps (Martin et al. 2007) occurred at later postlarval stages, posteriorly to the development of epipodites. Further work is needed to understand the morphological and physiological adaptations of *L. vannamei* allowing its life in a benthonic habit of coastal lagoons or estuaries during postlarval stages.

Ontogeny of the osmoregulatory function

In a previous study on the ontogeny of osmoregulation of *L. vannamei* (Chong-Robles et al. 2014), we have shown that mysis larvae are close to osmo-conformation with low osmoregulatory (OC) capacity at low and high salinities; OC progressively increases in postlarval stages and reaches its maximum value in juveniles and adults. Our present results regarding the ontogeny of the branchial osmoregulatory organs can be connected with these physiological events.

Even as branchial chambers begin to develop in larval stages, we did not find ionocytes or NKA expression in any structure of the branchial chambers of *L. vannamei* during larval stages. This is different from some other decapod species. For example, ionocytes with NKA expression (ionocytes type 2) are present in the pleura and branchiostegites in zoea I stage of *C. crangon* (Cieluch et al. 2005) and in all structures forming the branchial chambers and in the antennal glands of the freshwater prawn *M. amazonicum* during zoea stages (Boudour-Boucheker et al. 2013); both of these species are able to efficiently osmoregulate at these early stages. In contrast, we report here the lack of NKA expression during larval stages in gills, branchiostegite, and pleura, consistent with the lack of ionocytes in the pleura and branchiostegite in the mysis stage. Obviously, the different organs of the branchial chamber are not involved in any ion transport activity in the larval stages of *L. vannamei*. These larvae live in seawater (Dall et al. 1991), thus under rather constant salinity in which they are isosmotic to this medium (Chong-Robles et al. 2014).

In the PL1 stage, we found ionocytes developed in the epithelia of the inner side of the branchiostegites and in the first epipodite. At this stage, there is a change in the pattern of osmoregulation, as the young shrimps begin to slightly hyper-hypo osmoregulate depending on the surrounding salinity (Chong-Robles et al. 2014). The ionocytes observed at the PL1 stage present typical structural features including basal membrane infoldings, several mitochondria, and evaginations in their apical membrane, but no NKA immunostaining was observed in these cells in PL1, PL2, and PL4. The animals used in these experiments had been maintained in seawater (32 PSU) in which they are almost isosmotic to the external medium with only very slight hypo-regulation. This weak osmoregulatory activity may be associated with a low expression of NKA then undetectable through IIF. Further observations conducted at lower and higher salinities, prompting stronger osmoregulation, would be useful. Similar ultrastructure of ionocytes has been observed in branchiostegites and epipodites in postlarvae of *P. japonicus* (Bouaricha et al. 1994), but without data about the NKA localization. To our knowledge, NKA localization in larval stages of a penaeid shrimp has only been reported in *L. stylirostris*, but the cell ultrastructure of ionocytes was only observed until PL9 (Pham et al. 2016). In other species, NKA expression was visualized in postlarvae in at least one structure of the branchial chamber involved in osmoregulation: for instance in the 1st decapodite of *C. crangon* (Cieluch et al. 2005) and *M. amazonicum* (Boudour-Boucheker et al. 2013) and in postlarvae IV of *H. gammarus* (Lignot et al. 1999).

In *L. vannamei*, NKA was detected in ionocytes from the PL15 stage. At this stage, the ionocytes present in epipodites and on the inner side of the branchiostegites had a more developed basolateral membrane infolding system, while the apical evaginations in the ionocytes of epipodites had a similar development compared to those observed in the PL1. NKA was specifically localized on the basolateral side of the ionocytes. Similar observations have been reported in *C. crangon* (Cieluch et al. 2005), *M. amazonicum* (Boudour-Boucheker et al. 2013), *H. gammarus* (Lignot et al. 1999), *L. stylirostris*

(Pham et al. 2016), and *Scylla paramamosain* (Chung and Lin 2006). In gills, the cells did not show any ultrastructure typical of ionocytes, and no evidence of NKA was found through IIF. And we did not detect any change in the localization of the osmoregulatory function during the development as reported in other decapod species (Bouaricha et al. 1994; Lignot and Charmantier 2001; Cieluch et al. 2005; Boudour-Boucheker et al. 2013; Pham et al. 2016).

The function of epipodites and of the inner side of the branchiostegites as the main osmoregulatory structures has also been recognized in *P. japonicus* (Bouaricha et al. 1994), *L. stylirostris* (Pham et al. 2016), *C. crangon* (Cieluch et al. 2005), *H. gammarus* (Lignot and Charmantier 2001), and *Rimicaris exoculata* (Martinez et al. 2005). In these species, these osmoregulatory organs are active as soon as they emerge, for instance in embryos (Lignot and Charmantier, 2001), or in larval or first postlarval stages (Bouaricha et al. 1994; Pham et al. 2016). In contrast, ionocytes of the branchiostegite and epipodite of *L. vannamei* are involved later in osmoregulation. The fact that gills are not involved in osmoregulation, but rather in respiration, as we propose in *L. vannamei*, has been previously reported in *Homarus gammarus* (Lignot and Charmantier 2001), *P. japonicus* (Bouaricha et al. 1994), *Rimicaris exoculata* (Martinez et al. 2005), and *L. stylirostris* (Pham et al. 2016). Our finding is promising and could be explored with more specific single-cell studies, and under the hyper-osmoregulatory behavior, which were out of our scope.

From molecules to the environments, an integrated series of events links osmoregulation to the habitat of a species at each developmental stage. The expression of specific transporters such as NKA, coordinated with the structural development of ionocytes at several anatomical sites, result in stagespecific levels of osmoregulation; they in turn determine the salinity tolerance of the successive ontogenetical stages which is a parameter of their selection and adaptation to habitats (Charmantier et al. 2009). In other terms, the development of animals is associated with physiological changes necessary to survive at each phase of their live (Anger 2006). The osmoregulatory specialization found at the organ, cellular, and molecular levels in *L. vannamei* is in agreement with their osmoregulatory pattern, their salinity tolerance, and their changes in habitats (Chong-Robles et al. 2014). The presence of osmoregulatory epithelia in branchiostegites and epipodites from the PL1 stage and the activation of molecular mechanisms based on NKA from PL15 suggest that these are key developmental stages during their life cycle. In penaeid shrimps, the larvae and early postlarvae stages, that possess a limited ability to osmoregulate, are adapted to live in oceans where seawater salinity is generally stable; then, after larval development, the animals become benthic postlarvae ready for recruitment to coastal lagoons and estuaries (Mair et al. 1982).

Although in this study we used animal reared in aquacultural ponds, the evaluated sizes of PL1 to PL22 stages (5 ± 0.005–12 ± 0.33 mm; Chong-Robles et al. 2014) are similar to those reported in the recruitment to the Bahía Salinas del Marqués, Oaxaca (Rámos-Crúz and Rámos-Santiago 2006). It could be possible that *L. vannamei* during ontogeny developed first an adaptation to low salinity and posteriorly with the development of all epipodites, an adaptation to high salinity. Future work should focus on the effect of low salinity (or under hyper-osmoregulatory behavior) on the activity and function of NKA and of other transporters such as V-type H^+-ATPase, which play an important role in the hyper-osmoregulation (Boudour-Boucheker et al. 2014). Also, the specific contribution of each anatomical/cellular structure, including antennal gland, under different salinities remains to be determined.

Acknowledgements We wish to thank the Laboratory of Histology of the Sciences Faculty and Laboratory of Macroalgae of Institute of Oceanographic Research at Autonomous University of Baja California, Mexico. We appreciate the support of Dr. Rosa Mouriño from the Department of Microbiology, Center for Scientific Research and Higher Education of Ensenada (CICESE), Mexico, for the facilities to use the epifluorescence microscope. Thanks also due to the National Laboratory of Nanoscience and Nanotechnology Research (LINAN) from the Institute for Scientific and Technological Research of San Luis Potosi (IPICyT), Mexico, for the facilities to use the transmission electron microscopy and to Araceli Patrón from Molecular Biology DivisionLINAN-IPICYT for the SEM and TEM morphology characterizations. Finally, we are very thankful to the staff of AQUAPACIFIC company for their invaluable support to obtain each developmental stage of *L. vannamei* for this investigation.

Funding This project was funded by CONACyT—Ciencia básica I0110/194/09 allocated to IGM and a PhD grant 184694 to JCR.

Declarations

Ethical approval All applicable international, national, and/or institutional guidelines for the care and use of animals were followed.

Conflict of interest The authors declare no competing interests.

Figure 1

Branchial chamber development of *L. vannamei*. **a** Methylene blue staining at zoea stage. Note the lack of gills and epipodites; **b** scanning electron microscopy of gills in PL1 stage. Note the development of a few incipient gills in the form of a tube inside the branchial chamber cavity; **c** methylene blue staining of gills and epipodites at PL4 stage; **d** methylene blue staining of gills and epipodites at PL10. Note the epipodites and buds of epipodites developed at these stages and the last pleurobranch gill; **e** scanning electron microscopy of gills in PL15 stage. Note the incipient ramification in an arthrobranch gill (arrow); **f** adult *L. vannamei* fixed with Davidson's solution show the five epipodites completely developed (delimited by dotted line). E, epipodite; G, gills; M, maxilliped; P, pereiopods

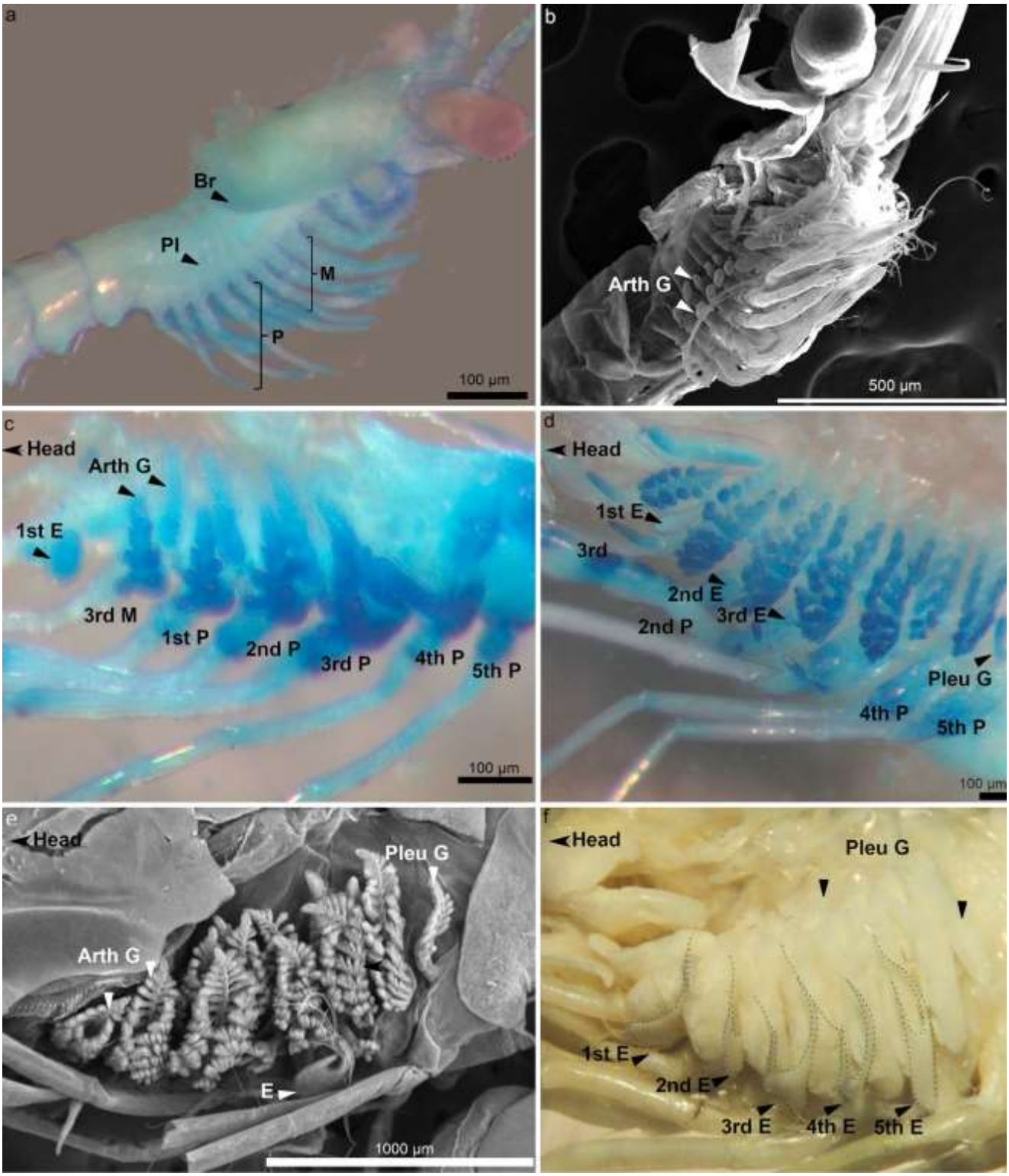

Figure 2
Hematoxylin and eosin staining shows the early branchial chamber development in *L. vannamei* at the mysis stage. Note the incipient septum in gills (arrow). Br, branchiostegite; Arth G, arthrobranch gills; Pl, pleura; C, cuticle; Ec, external cuticle; Ic, internal cuticle

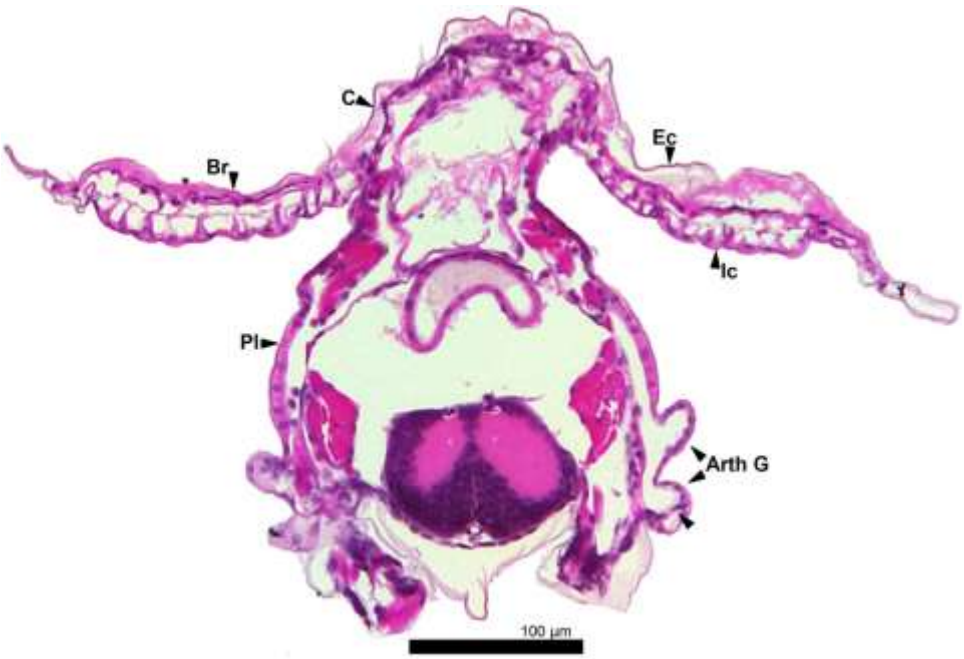

Figure 3

Hematoxylin and eosin staining of the branchiostegite in *L. vannamei*. **a** PL15; **b** PL39, and **c** juvenile. Note the different epithelial cells forming each side of the structure and how the cells forming the internal epithelium became more like prismatic cells at the juvenile stage; **d** hematoxylin and eosin staining of the epipodites at PL1 stage; **e** PL15; and **f** juvenile. Note the same epithelial cells around the structure and how they become more prismatic at the juvenile stage. C, cuticle; H, hemolymph; N, nucleus; Ec, external cuticle; Ee, external epithelium; Ic, internal cuticle; Ie, internal epithelium

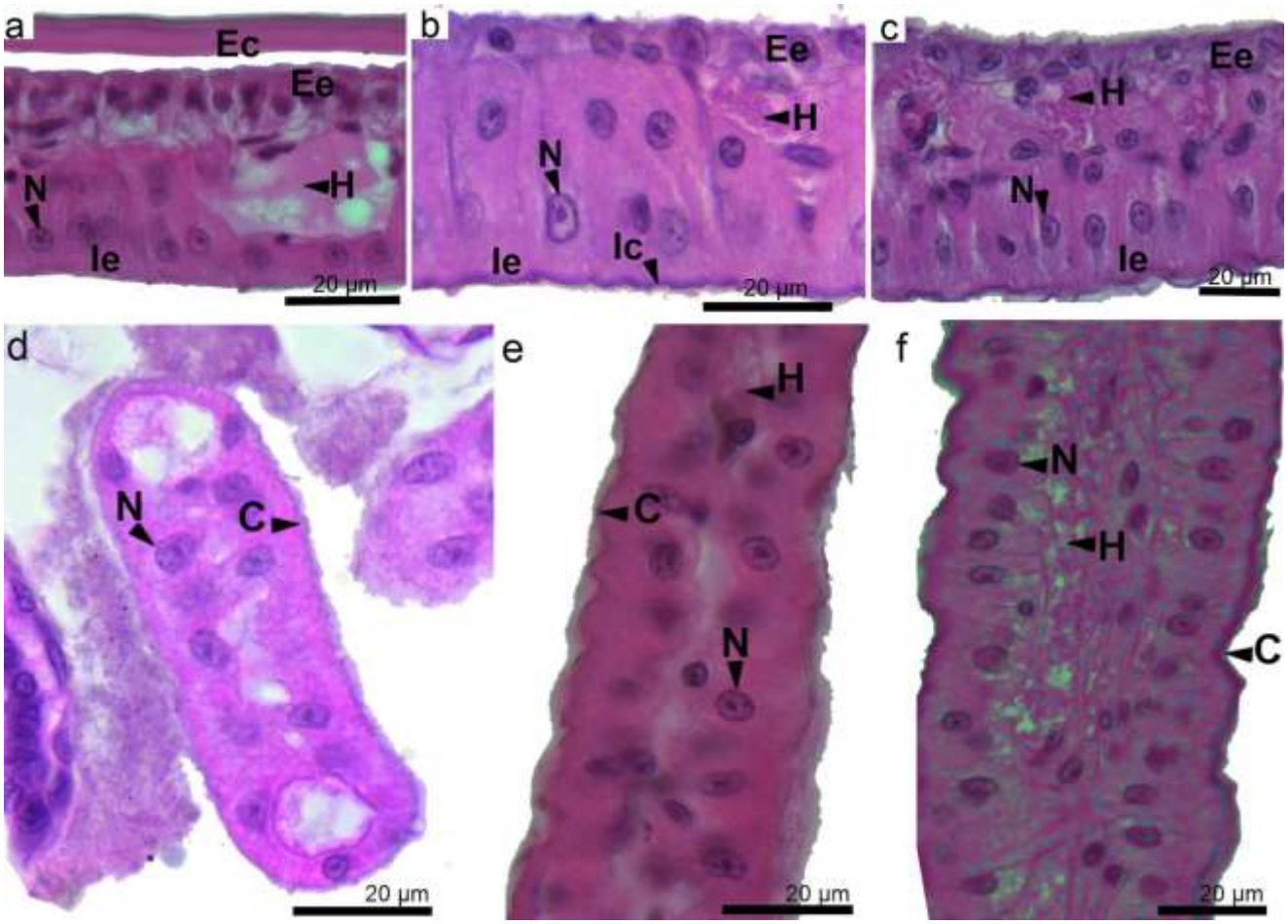

Figure 4

Schematic representation of a transverse section of a branchial chamber in key developmental stages of L. vannamei. a Transversal section of the shrimp; b represent zoea stage. Note the space of the branchial chamber (shading); c represent mysis stage; d represent PL1 stage; e represent PL4 stage; f represent a PL10 stage with epipodites developed (see Fig. 1d); g represent the branchial chamber since PL15 stage. Br, branchiostegite; Arth G, arthrobranch gills; P, pereiopods; Pl, pleura; Pleu G, pleurobranch gills. Created with BioRender.com

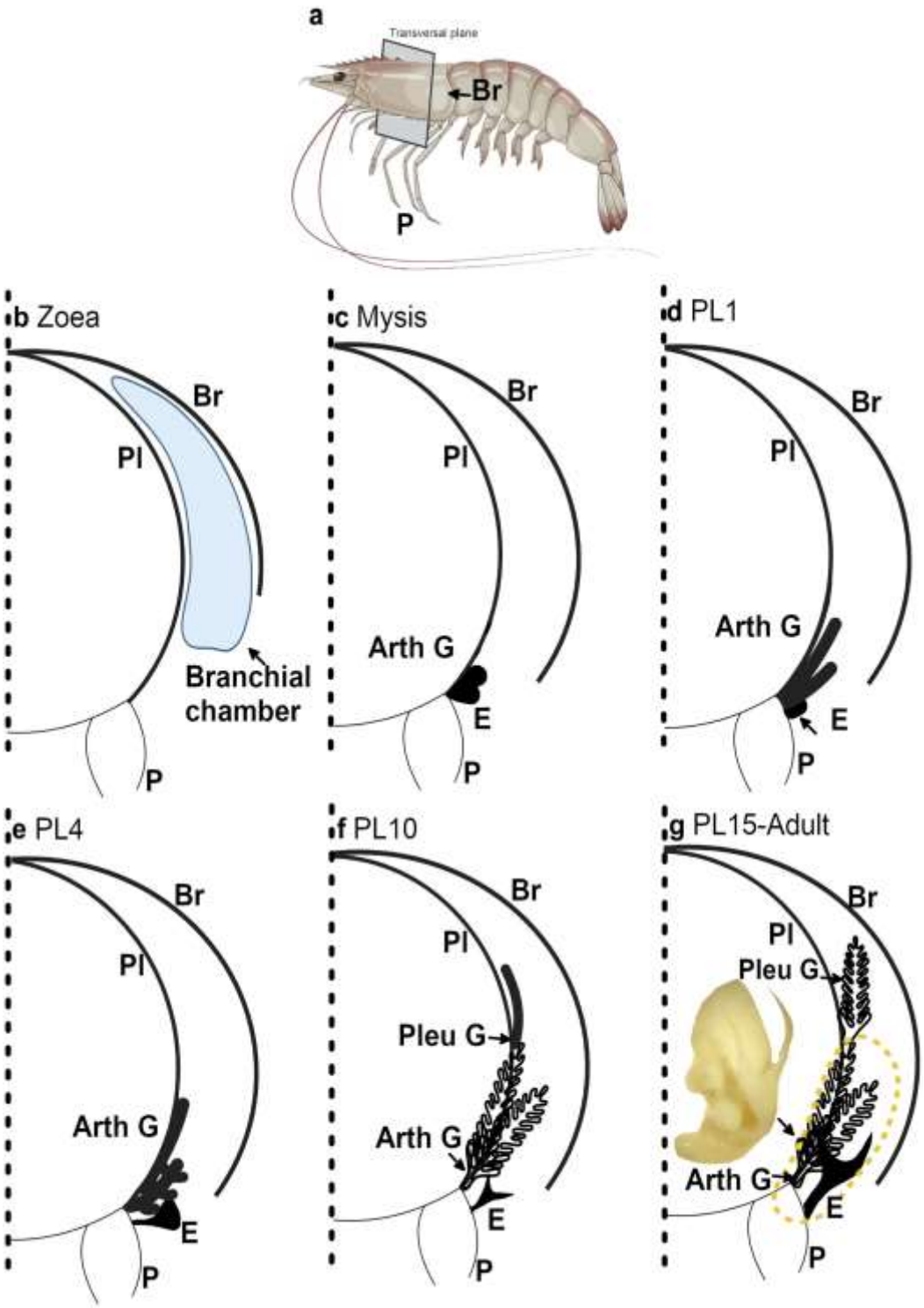

Figure 5

Branchial chamber of the mysis stage of *L. vannamei*. **a** Immunolocalization of Na^+, K^+ -ATPase; **b** transmission electron micrograph of pleura; **c** transmission electron micrograph of branchiostegite. Note the absence of fluorescence in the branchiostegite, pleura, and gills bud (**a**) and the cell ultrastructure without ion transport related features (**b**, **c**). Br, branchiostegite; C, cuticle; Ec, external cuticle; Ee, external epithelium; Gb, gill buds; Ic, internal cuticle; Ie, internal epithelium; Pl, pleura; N, nucleus

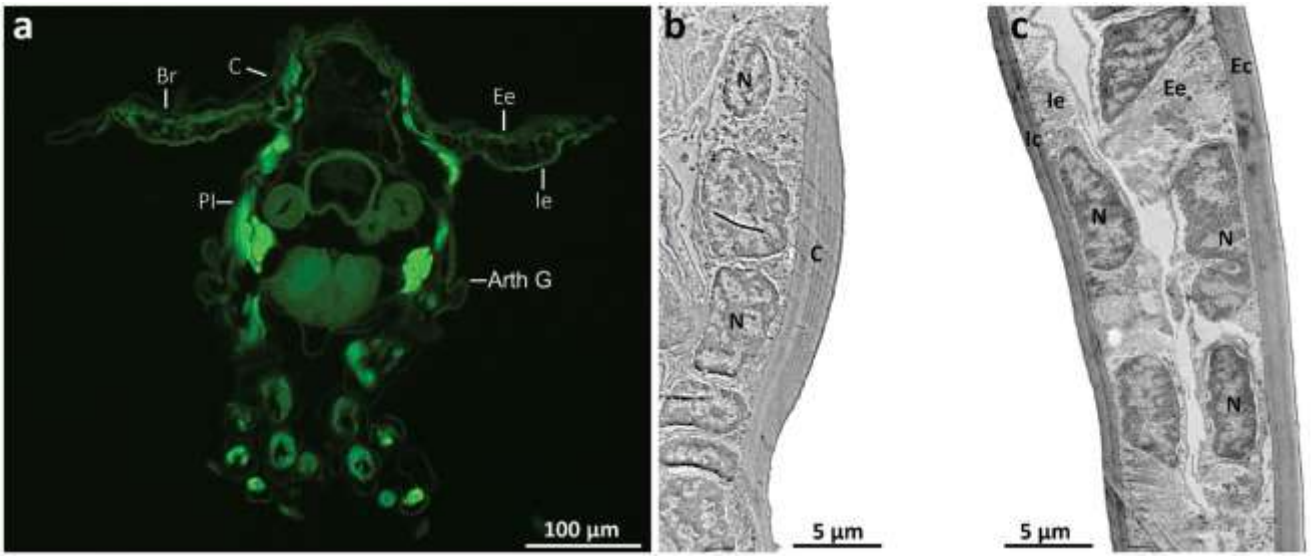

Figure 6

Transmission electron micrographs of the branchial chamber of *L. vannamei*. **a** External epithelium of branchiostegite at PL1 stage showing the cubic epithelium below a thick cuticle and the basal invaginations of ionocytes of the internal epithelium; **b** internal epithelium of branchiostegite at PL1 stage showing the perpendicular apical evaginations of ionocytes associated with the thicker cuticle; **c** pilaster cell at PL1 stage joining the two facing epithelia; **d** epipodite at PL1 stage showing the epithelium formed by ionocytes with a lot of mitochondria and evaginations in close contact with the cuticle; **e** internal side of branchiostegite at PL15 stage showing typical ionocytes with basal infoldings associated with mitochondria and apical evaginations associated to the thick cuticle of the internal side of the structure; **f** close up of the basal side of ionocyte showing many mitochondria associated as a "mitochondria pump" (shading); **g** close up of the inner side of the branchiostegite showing an extensive apical evaginations zone of the ionocyte; **h** ionocytes from the epipodite at the adult stage with a few apical evaginations and basal infoldings; **i** close up of the ionocytes at adult stage showing the basal infolding associated to mitochondria. Ae, apical evaginations; Bi, basal infolding; Bm, basal membrane; C, cuticle; Ec, external cuticle; H, hemolymph; Ic, internal cuticle; M, mitochondria; N, nucleus

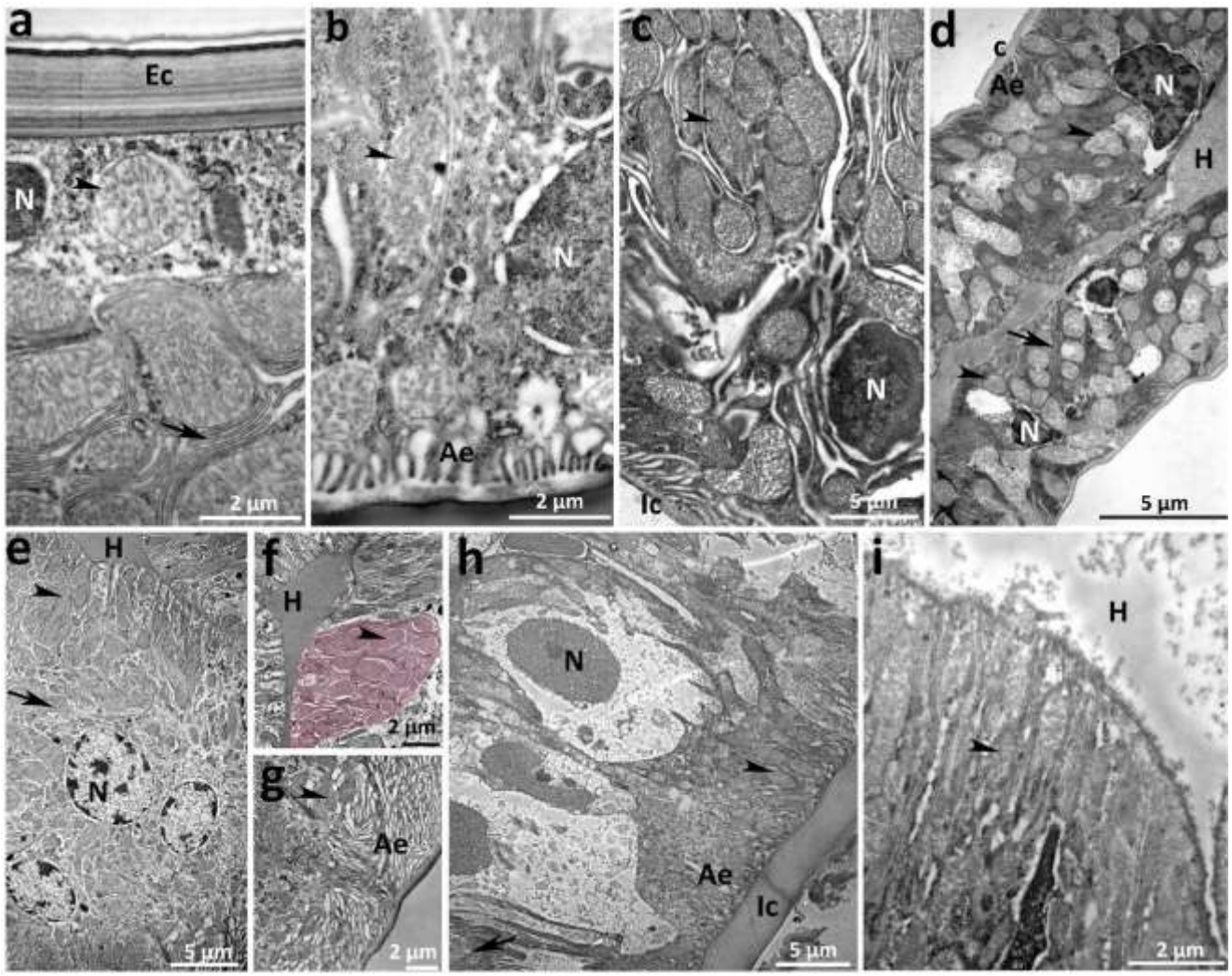

Figure 7

Immunolocalization of Na^+/K^+-ATPase in the branchial chamber of *L. vannamei*. **a** Branchial chamber of PL15; **b** branchial chamber of juvenile; **c** branchiostegite in juvenile; and **d** epipodite in juvenile. Arrow heads show the basolateral distribution of fluorescence. Note in both stages the absence of fluorescence in gill structures. Br, branchiostegite; E, epipodite; G, gills

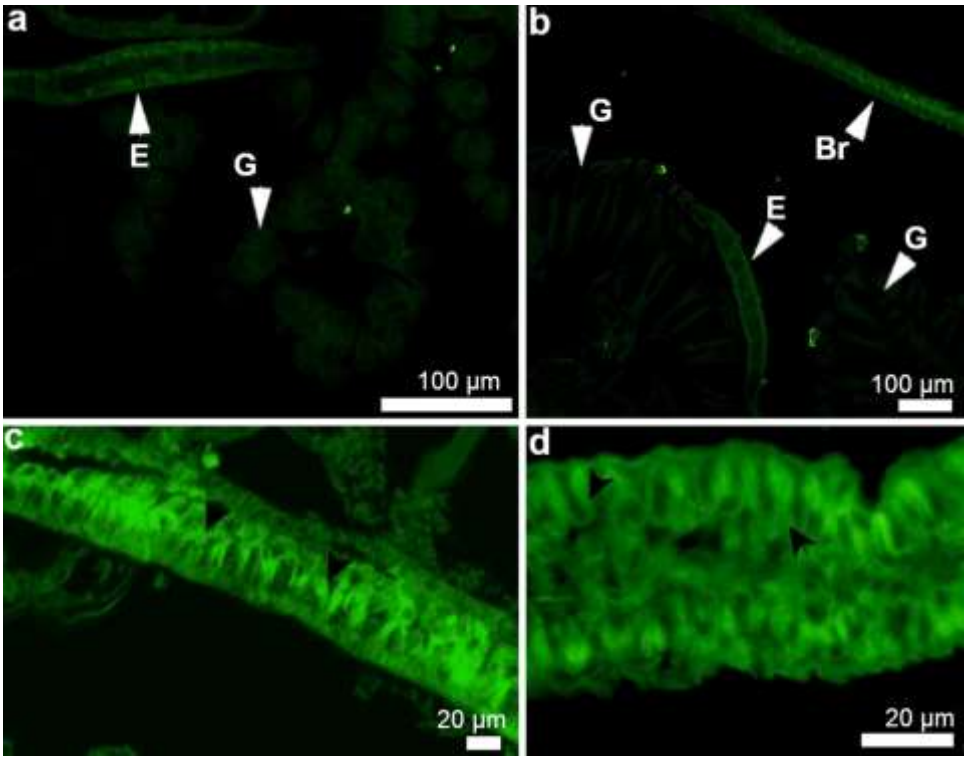

Figure 8
Transmission electron micrograph of the gills of *L. vannamei*. **a** Longitudinal section of secondary septum of PL15; **b** transverse section of secondary septum of a juvenile; **c** transverse section of lamella of juvenile. Note the flat cells without ionocyte features forming the structure. C, cuticle; H, hemolymph; N, nucleus; Ss, secondary septum

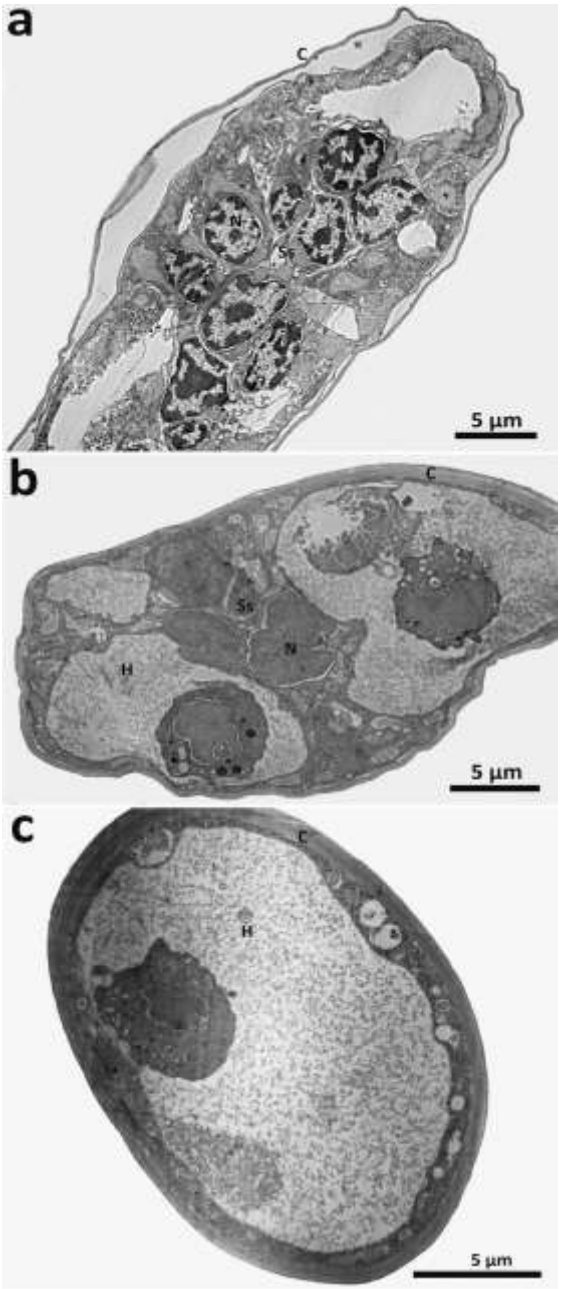

Table 1
Summary of *Litopenaeus vannamei* branchial chamber development

Structure	Developmental stage						
	Z3	M2 and M3	PL1	PL4	PL15	J	A
Pleura	-	-	-	-	-	-	-
Gill		-	-	-	-	-	-
Branchiostegite	-	-	-*	-	+*	+	ns
Epipodite			-*	-	+	+*	+*

Black boxes indicate that the structure is not developed at that stage

Z zoea, *M* mysis, *PL* postlarva, *J* juvenile, *A* adult, − absence of immunolabeling, + positive immunolabeling indicating presence of Na + /K + -ATPase, * ionocytes observed by TEM, ns not studied for TEM

References

Anger K (2001) The biology of decapod crustacean larvae. In: Crustacean Issues 14. Balkema, Lisse

Anger K (2006) Contributions of larval biology to crustacean research: a review. Invertebr Reprod Dev 49:175–205

Bauer RT (1999) Gill-cleaning mechanisms of a dendrobranchiate shrimp, *Rimapenaeus similis* (Decapoda, Penaeidae): description and experimental testing of function. J Morphol 242:125–139

Bouaricha N, Charmantier-Daures M, Thuet P, Trilles J, Charmantier G (1994) Ontogeny of osmoregulatory structures in the shrimp *Penaeus japonicus* (Crustacea, Decapoda). Biol Bull 186:29–40

Bouaricha N, Charmantier G, Charmantier-Daures M, Thuet P, Trilles J (1991) Ontogénèse de l'osmorégulation chez la cravette *Penaeus japonicus*. Cah Biol Mar 32:149–158

Boudour-Boucheker N, Boulo V, Charmantier-Daures M, Grousset E, Anger K, Charmantier G, Lorin-Nebel C (2014) Differential distribution of V-type H+-ATPase and Na+/K+-ATPase in the branchial chamber of the palaemonid shrimp *Macrobrachium amazonicum*. Cell Tissue Res 357:195–206

Boudour-Boucheker N, Boulo V, Lorin-Nebel C, Elguero C, Grousset E, Anger K, Charmantier-Daures M, Charmantier G (2013) Adaptation to freshwater in the palaemonid shrimp Macrobrachium amazonicum: comparative ontogeny of osmoregulatory organs. Cell Tissue Res 353:87–98

Charmantier G (1998) Ontogeny of osmoregulation in crustaceans: a review. Invertebr Reprod Dev 33:177–190

Charmantier G, Charmantier-Daures M, Towle D (2009) Osmotic and ionic regulation in aquatic arthropods. In: Evans D (ed) Osmotic and ionic regulation: cells and animals. Taylor and Francis, London, pp 165–208

Chong-Robles J, Giffard-Mena I, Charmantier G, Boulo V, LizárragaValdéz J, Enriquez-Paredes LM (2014) Osmoregulation pattern and salinity tolerance of the white shrimp *Litopenaeus vannamei* (Boone, 1931) during post-embryonic development. Aquaculture 422–423:261–267

Chung KF, Lin HC (2006) Osmoregulation and Na, K-ATPase expression in osmoregulatory organs of *Scylla paramamosai*n. Comp Biochem Physiol Part A Mol Integr Physiol 144:48–57

Cieluch U, Charmantier G, Grousset E, Charmantier-Daures M, Anger K (2005) Osmoregulation, immunolocalization of Na+/K+- ATPase, and ultrastructure of branchial epithelia in the developing brown shrimp, *Crangon crangon* (Crustacea, Decapoda). Physiol Biochem Zool 78:1017–1025

Cieluch U, Klaus A, Aujoulat F, Buchholz F, Charmantier-Daures M, Charmantier G (2004) Ontogeny of osmoregulatory structures and functions in the green crab *Carcinus maenas* (Crustacea, Decapoda). J Exp Biol 207:325–336

Dall W, Hill BJ, Rothlisberg PC, Sharples DJ (eds) (1991) Life histories. In: The biology of the penaeidae. Academic Press, pp 283–314

FAO (2004) Manejo sanitario y mantenimiento de la bioseguridad de los laboratorios de postlarvas de camarón blanco (*Penaeus vannamei*) en América Latina. FAO Doc Técnico Pesca 450:66

Freire CA, Onken H, McNamara JC (2008) A structure-function analysis of ion transport in crustacean gills and excretory organs. Comp Biochem Physiol - Part A Mol Integr Physiol 151:272–304

Gilles R, Pequeux A (1981) Cell volume regulation in crustaceans: relationship between mechanisms for controlling the osmolality of extracellular and intracellular fluids. J Exp Zool 215:351–362

Kitani H (1986) Larval development of the white shrimp *Penaeus vannamei* BOONE reared in the laboratory and the statistical observation of its naupliar stages. Bull Japanese Soc Sci Fish
52:1131–1139

Lightner DV (1996) A handbook of pathology and diagnostic procedures for diseases of penaeid shrimp. Baton Rouge, Louisiana, USA

Lignot J-H, Charmantier-Daures M, Charmantier G (1999) Immunolocalization of Na+/K+-ATPase in the organs of the branchial cavity of the European lobster Homarus gammarus (Crustacea: Decapoda). Cell Tissue Res 296:417–426

Lignot J-H, Charmantier G (2001) Immunolocalization of Na, K ATPase in the branchial cavity during the early development of the European lobster *Homarus gammarus* (Crustacea, Decapoda). J Histochem Cytochem 49:1013–1023

Mair JM, Watkins JL, Williamson D (1982) Factors affecting the immigration of postlarval penaeid shrimp into a Mexican lagoon system. Oceanol Acta, Spec issue

Mantel LH, Farmer LL, Gilles R, Pequeux A (1983) Osmotic and ionic regulation. In: Mantel LH (ed) The biology of Crustacea, vol 5. Internal anatomy and physiological regulation. Academic Press Inc, New York, London, pp 53–161

Martin JW, Liu EM, Striley D (2007) Morphological observations on the gills of dendrobranchiate shrimps. Zool Anz 246:115–125

Martinez AS, Charmantier-Daures M, Compère P, Charmantier G (2005) Branchial chamber tissues in two caridean shrimps: the epibenthic *Palaemon adspersus* and the deep-sea hydrothermal *Rimicaris exoculata*. Tissue Cell 37:153–165

McNamara JC, Faria SC (2012) Evolution of osmoregulatory patterns and gill ion transport mechanisms in the decapod Crustacea: a review. J Comp Physiol B Biochem Syst Environ Physiol 1–18

Péqueux A (1995) Osmotic regulation in crustaceans. J Crustac Biol 15:1–60

Péqueux A, Dandrifosse G, Loret S, Charmantier G, Charmantier-Daures M, Spanings-Pierrot C, Schoffeniels E (2006) Osmoregulation: morphological, physiological, bio-chemical, hormonal, and developmental aspects. In: Forest J, Klein J von V (eds) The Crustacea, vol 2. Brill, Leiden Boston, pp 205–308

Pham D, Charmantier G, Boulo V, Wabete N, Ansquer D, Dauga C, Grousset E, Labreuche Y, Charmantier-Daures M (2016) Ontogeny of osmoregulation in the Pacific blue shrimp, *Litopenaeus stylirostris* (Decapoda, Penaeidae): deciphering the role of the Na+/K+-ATPase. Comp Biochem Physiol Part - B Biochem Mol Biol 196–197:27–37

Pham D, Charmantier G, Wabete N, Boulo V, Broutoi F, Mailliez J-R, Peignon J-M, Charmantier-Daures M (2012) Salinity tolerance, ontogeny of osmoregulation and zootechnical improvement in the larval rearing of the Caledonian blue shrimp, *Litopenaeus stylirostris* (Decapoda, Penaeidae). Aquaculture 362–363:10–17

Rámos-Crúz S, Rámos-Santiago E (2006) Abundancia relativa de postlarvas de camarones penéidos en la Bahía Salinas del Marqués, Golfo de Tehuantepec, México. Marzo a Junio de 1999. Rev Biol Mar Oceanogr 41:121–128

Rodríguez-Pérez BP, Medina-Arredondo M, Escobeo-Bonilla CM (2006) Estadios de muda de camarones (*Litopenaeus vannamei*) adultos sanos y susceptibilidad al virus de mancha blanca (WSSV). In: VII Encuentro de Biotecnología. Mazatlán, Sinaloa. Octubre 11–13, 2010.

Taylor H, Taylor E (1992) Gills and lungs: the exchange of gases and ions. In: Harrison F, Humes A (eds) Microscopic anatomy of invertebrates, vol 10. Wiley-Liss Inc, New York, pp 203–293